Addressing Soft Rock Hazards: Case Studies of Sinkholes and Collapses in Faulted Limestone Strata

Seokwon Jeon

Seoul National University, Seoul, Republic of Korea

Abstract: Soft rock formations, particularly faulted and fractured limestone strata, are susceptible to ground subsidence and collapse, posing significant geohazard risks in mining regions. This paper presents two case studies from South Korea that exemplify the complex interplay between geological conditions, anthropogenic excavation, and surface deformation. The first case focuses on a large-scale subsidence event at the Uljin limestone mine, where subsurface cavities, developed along faulted and karstified limestone zones, were found to be the primary cause of surface sinkholes. Geophysical surveys, borehole investigations, and three-dimensional numerical modeling confirmed that past mining operations intersected with natural weak zones, resulting in progressive ground instability. The second case examines the Yemi Mountain area, where sequential surface collapses and slope failures occurred in a zone underlain by old mine workings and structurally weakened carbonate rocks. Detailed analyses, including resistivity surveys, drilling, and mechanical testing, identified fault gouge zones and degraded rock mass conditions that contributed to localized instability. In both cases, the sinkholes were exacerbated by the presence of highly weathered soft rocks and insufficient separation between underground voids and the surface. The findings underscore the need for comprehensive characterization of soft rock behavior, particularly in faulted terrains, and for improved monitoring of abandoned mine areas. The results highlight the importance of integrating geological, geophysical, and geomechanical data in the assessment of soft rock hazards and suggest mitigation strategies tailored to the lithological and structural context of the affected sites.

Keywords: Soft Rock Hazards, Faulted Limestone Strata, Sinkholes and Collapses, Geomechanical Assessment

1. Introduction

Soft rocks, typically defined by their low strength, high deformability, and susceptibility to weathering, are known to pose significant geotechnical challenges in underground construction and surface stability assessment. When such rocks are intersected by structural discontinuities such as faults and joints, and are subjected to anthropogenic disturbances—especially mining activities—they become especially prone to subsurface collapse and associated surface deformation. In particular, limestone terrains with fault-induced fracturing and karst features represent a category of soft rocks with elevated geohazard potential, as documented in numerous studies.

Ground subsidence and sinkhole formation in these geological settings are often triggered by the presence of underground cavities—both natural and man-made—that undergo progressive enlargement due to mechanical deterioration and water infiltration. These failures are sometimes sudden and catastrophic, particularly when the overburden is insufficient or weakened by surface loads or dynamic events. Such events not only threaten infrastructure and human life but also reveal the complexity of predicting failure behavior in structurally compromised soft rock systems.

In South Korea, the interplay between faulted limestone geology and historical underground mining has led to multiple

subsidence disasters. This presentation focuses on two case studies: one from the Uljin limestone mining area and the other from the Yemi Mountain area where an iron mine is located. The Uljin limestone mine employed the room-and-pillar mining method, whereas H Mine in Mt. Yemi utilized the caving method. In both cases, underground collapses occurred in areas where abandoned or inactive mine cavities overlapped with faults and karst features. The Uljin case involved the collapse of surface areas above mine workings where no adequate geological separation remained, while the Yemi case featured sinkholes and slope failures influenced by subsurface voids, natural faults, and karst cavities.

A detailed investigation of the Uljin area (KIGAM, 2017) confirmed that the deeply weathered limestone affected by faulting showed a sharp reduction in shear strength and that only a thin layer of residual ground remained above the cavities. Electrical resistivity surveys, borehole investigations, and laboratory tests identified weak zones consistent with the collapse locations.

In the Yemi case, investigations revealed that abandoned mine voids were connected to fault gouge zones and fractured limestone. Drone-based topographic modeling and stress reduction analysis demonstrated that time-dependent deformation and rock bridge failures led to eventual surface collapse.

These analyses underscore the heterogeneity, uncertainty, and predictive challenges associated with soft rock behavior. An integrated approach—combining geophysical surveys, in-situ testing, and numerical modeling—is essential for reliable hazard evaluation.

This study aims to identify risk factors associated with faulted weak rock conditions through real collapse cases and proposes hazard assessment and mitigation strategies by integrating geological, geotechnical, and mining-related data. The structure of the presentation is as follows: Chapter 2 explains the investigation methodology and scope, including electrical resistivity survey, borehole drilling, and laboratory testing; Chapter 3 compares and analyzes the field findings from the two case studies; Chapter 4 discusses implications for instability in weak rock grounds; Chapter 5 presents the conclusions and future directions.

2. Investigation Methods and Scope

In both cases, a multi-faceted investigation approach was applied to identify the causes of subsidence and collapse in weak limestone ground. Methods included geological surveys, geophysical prospecting, borehole drilling and laboratory testing, and analysis of mining records. The investigation was conducted independently at two different sites (Uljin and Mt. Yemi), both of which showed influences from fault development, karstic voids, and past mining activity.

2.1 Surface Geological and Topographic Survey

The investigation included geological mapping of the surface, fault exposure surveys, and satellite/aerial photo analysis. For the Uljin case, the focus was not on stratigraphic investigation but rather on characterizing the lithological units present in the study area, to aid in identifying collapse causes and formulating countermeasures. From bottom to top, the rock units were identified as crystalline limestone, quartzite, and interbedded limestone and slate.

Similarly, in the Mt. Yemi case, lithological characteristics rather than stratigraphy were examined. In addition, a drone-based (UAV) topographic survey was conducted. The drone imagery was processed into orthophotos and 3D models, which were then used to analyze the spatial distribution and magnitude of surface subsidence.

2.2 Geophysical Surveys

In the Uljin case, electrical resistivity surveys were conducted with the following objectives:

- Identify the distribution of fault zones and weak geological formations associated with NE-SW structural trends.
- Determine the extent of collapse and subsidence in the Uljin and Namsusan mining areas.
- Evaluate the distribution and depth of geological structures and limestone voids associated with sinkhole development.

Three survey lines were set in the NE-SW direction parallel to the Songchon Fault, a major geological feature in the area, and another three lines in the SE-NW direction perpendicular to it. Among these, two lines were designed to pass through fractured zones and one through an unfractured zone to assess the effects of ground discontinuities on deformation. Figure 1 illustrates the location of the electrical resistivity survey lines.

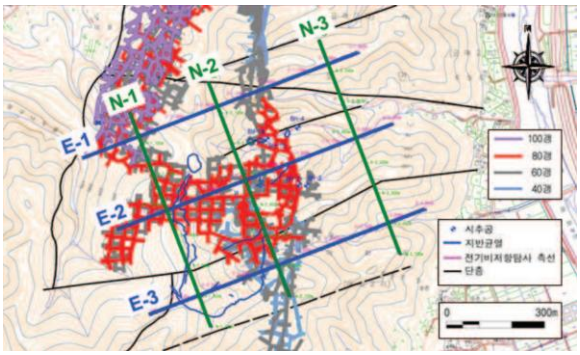

Figure 1. Location map of electrical resistivity survey lines

In the Yemi case, the survey lines passed directly beneath the surface subsidence zone. Based on surface geology, the fault strikes were identified as NNE, and surface cracks predominantly developed in the N-S direction. Thus, Line-1 (NE-SW, 760 m), Line-2 (E-W), and an additional Line-3 (NW-SE) were surveyed as shown in Figure 2..

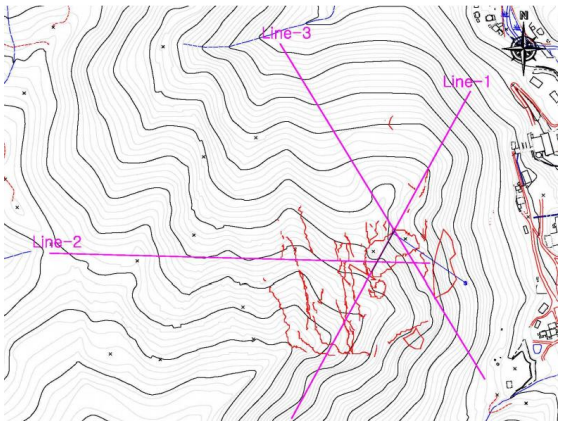

Figure 2. Electrical resistivity survey lines in the Yemi case

2.3 Borehole Drilling and Rock Core Logging

In the Uljin case, a total of five boreholes were drilled, including both inclined and vertical boreholes, to investigate the relationship between the subsidence boundary and underlying mine voids. Inclined drilling was specifically designed in direction and angle to intersect the predicted locations of subsidence and underground mine workings.

Voids were encountered in four of the five boreholes. The height of the voids was approximately six meters, consistent with the dimensions of mine tunnels, suggesting that the encountered voids were likely abandoned mine entries. Borehole cameras were used to acquire detailed visual data. The voids were identified as part of Level 60 and Level 80 in the Uljin limestone mine.

In the Yemi case, at Point B, two boreholes were drilled as shown in Figure 3: one horizontal borehole (BH-1) oriented N55W toward the lowest point of the primary subsidence area to investigate subsurface conditions and the boundary between the Hongjeom Formation and limestone, and one 40° inclined borehole (BH-2, 240 m long) designed to explore karst development within the limestone where past mining activity was suspected.

Borehole cores revealed core loss and fault breccia directly beneath the surface subsidence zone. In BH-2, continuous limestone and dolomite were recovered, and numerous small-scale (less than 1 m) dissolution cavities were observed. These findings suggest that faulted zones and small karstic cavities, in combination with past mining activity, likely contributed to the surface collapse.

Figure 3. Borehole locations in the Yemi case

2.4 Laboratory Testing

In the Uljin case, physical and mechanical properties of the rock and joint shear characteristics were determined from core samples collected in the five boreholes. Table 1 summarizes these properties. Average joint parameters were: cohesion 0.17 MPa, friction angle 29.8°, normal stiffness 62.3 GPa/m, shear stiffness 6.8 GPa/m, and dilation angle 12.5°.

In the Yemi case, average values for strength parameters were: uniaxial compressive strength 92 MPa, Young's modulus 45 GPa, Poisson's ratio 0.23, cohesion 15 MPa, internal friction angle 47°, and tensile strength 7.8 MPa.

Table 1. Physical and mechanical properties of rocks at Uljin

Property	Min	Max
Density (g/cm³)	2.58	2.71
Compression Strength (MPa)	33	171
Tensile Strength (MPa)	2	8
Young's Modulus (GPa)	26.1	62.6
Poisson's Ratio	0.09	0.27
Cohesion (MPa)	8	25
Internal Friction Angle (°)	36	54
mi (Hoek-Brown parameter)	9.358	18.644
σ_{ci} (MPa)	46.2	93.1

2.5 Analysis of Production History

Historical mine maps, cross-sections, and production records were reviewed to reconstruct the location and extent of underground voids. In the Uljin case, four mining levels existed between elevations of 40 m and 100 m above sea level, with several mined sections intersecting fault zones. Between 2015 and 2016, monthly limestone production ranged from 60,000 to 70,000 tons.

In the case of the Yemi site, the production history is complex. Development began in 1938, with initial mining focused on lead and zinc. From 1984 onward, iron ore was identified in the lower levels and has been actively mined to the present day. Lead and zinc ore bodies were mainly extracted between the 430ML and 603ML levels, while iron ore has been mined below the 385ML level. It has been reported that a total of 67,200 tons of zinc was produced between 1943 and 1983, and approximately 7.6 million tons of iron ore have been produced since 1984.

3. Case Analysis

This chapter presents detailed field investigation results, collapse patterns, and failure mechanisms for the Uljin limestone mining area (Case A) and the Mt. Yemi area (Case B). Both cases are located in faulted limestone zones where surface collapse occurred following past room-and-pillar or caving mining operations, without proper rehabilitation or monitoring.

3.1 Case A: Subsidence at the Uljin Limestone Mine

The Uljin limestone mine previously operated an open-pit site for high-grade raw material production. However, since 1995, large-scale underground mining tunnels—referred to as Levels 40, 60, 80, and 100 (named according to elevation above sea level)—have been developed to extract limestone for steelmaking and desulfurization purposes. Figure 4 presents the layout of mine tunnels at the Uljin Mine.

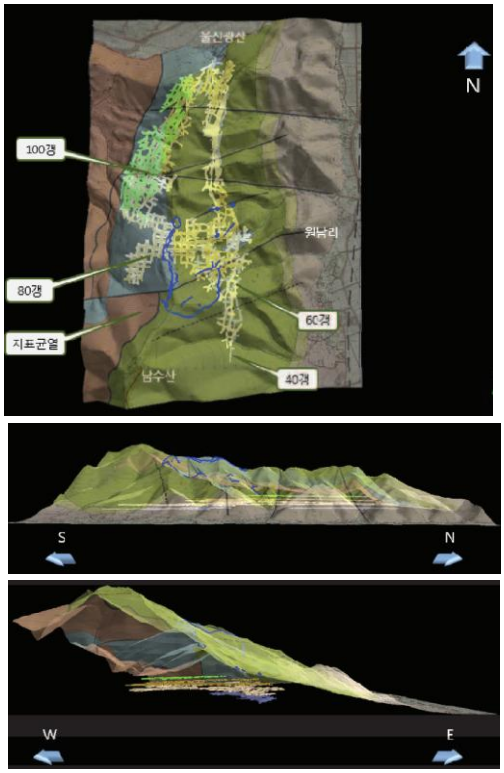

Figure 4. Layout of Mine Tunnels at the Uljin Limestone Mine

Between 2007 and 2016, the area around Mt. Namsu (EL 438 m) experienced a subsidence zone approximately 500 meters in its long axis and 250 meters in its short axis, covering an area of about 30,000 m² (13 hectares). The subsidence took the form of a collapse depression accompanied by tension cracks. Four sinkholes—likely associated with nearby faults—occurred along the northern boundary of the subsided zone, and a long, large-scale collapse depression extended northward along the ridge from the summit of Mt. Namsu (Figures 5 and 6).

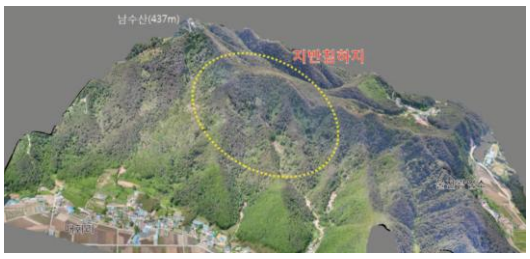

Figure 5. Location of Ground Subsidence in Uljin

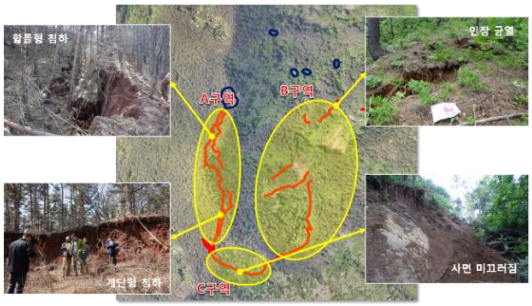

Figure 6. Current Status of Ground Subsidence in Uljin

The surface manifestations of ground subsidence show different characteristics by zone: in Zone A, collapse-type and step-like subsidence occurred; in Zone B, numerous tension cracks were identified; and in Zone C, slope sliding was observed. These types of subsidence differ from the trough-shaped subsidence typically caused by over-excavation and resemble subsidence induced by geological factors. Moreover, little vertical displacement was observed within the boundaries of the subsided area, and no cracks were found between the northern ends of Zones A and B. This suggests that no tunnel collapse occurred directly beneath the center of the subsided area that could explain the surface deformation. Thus, based on surface observations, no correlation can be drawn between the subsidence and over-excavation.

The investigation confirmed that the initial collapse occurred at the boundary between crystalline limestone and bedded limestone. This area corresponds to the major collapse zone shown on the level maps for Levels 60 and 80. These Levels were excavated through comparatively competent rock within a weak zone, likely to access the eastern ore body.

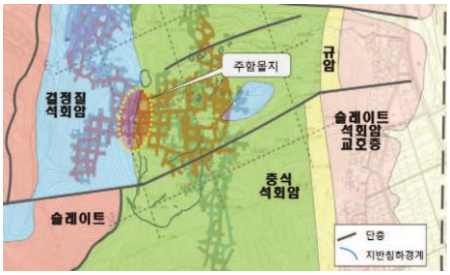

Figure 7. Geology Around the Main Collapse Zone

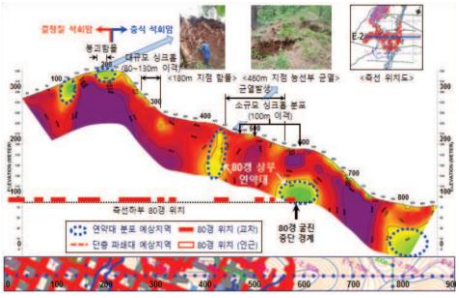

Figure 8. Electrical Resistivity Survey Results Across the Main Collapse Zone

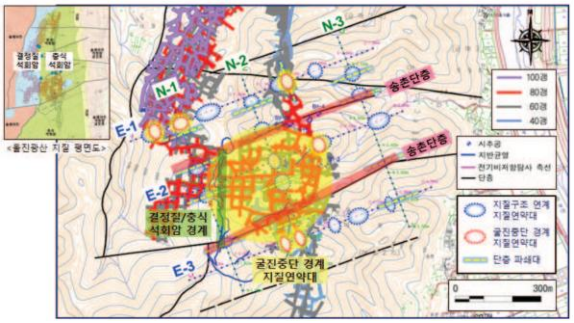

Figure 9. Plan View of Electrical Resistivity Anomalies

The electrical resistivity survey conducted across the main collapse zone in the east-west direction revealed a low-resistivity anomaly from 180 to 200 meters at depths of up to 20 meters as shown in Figures 8 and 9, with relatively higher resistivity values below. Levels 60 and 80, which run east-west, pass through this zone. This suggests that this section had better rock quality than surrounding areas, allowing excavation across the weak zone.

However, this area corresponds to the boundary between crystalline limestone and bedded limestone, where excavation may have exposed weak rock zones. Infiltration of rainwater likely led to weathering of the limestone, resulting in reduced shear strength of the rock.

A 2D numerical simulation using UDEC was conducted, incorporating the collapse of overlying rock above the mined voids, the presence of steep discontinuities, nearby faults, and limestone cavities found within 100 m of the surface as presented in Figure 10 and 11. The simulation results matched well with the observed slope failure and sinkhole development, indicating that geological weak zones such as faults and karstic cavities played a major role in the ground subsidence.

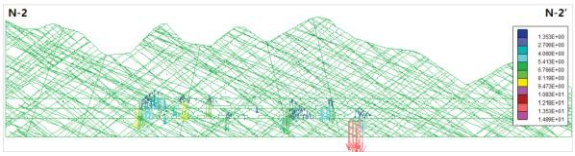

Figure 10. Distribution of Displacement in the Rock Mass

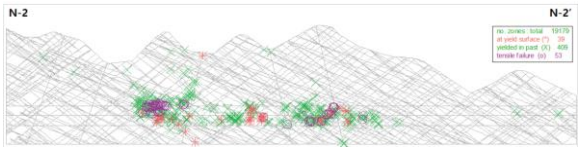

Figure 11. Distribution of Plastic Zones in the Rock Mass

In summary, the area where mine collapse and large-scale surface subsidence began coincides with the boundary between crystalline and bedded limestone, which is underlain by weak rock. Mine inspections showed that the rock surfaces on the tunnel crown were widely coated with clay-like materials, indicating weathering caused by rainwater infiltration, which likely reduced the rock's shear strength. On the surface, large-scale collapse and step-like subsidence occurred, accompanied by concentric cracking—typical signs of subsidence due to underlying weak geological zones.

Taken together, these findings suggest that discontinuities, faults, and karst cavities—representing geological weak zones—were the primary factors contributing to ground subsidence in the study area. This conclusion is further supported by the fact that 3D numerical modeling that did not account for geological weak zones predicted no surface collapse, whereas 2D modeling that included these features did predict surface failure.

3.2 Case B: Subsidence in the Mt. Yemi Area

The H Iron Mine at Mt. Yemi began development in 1938. Initially, lead and zinc were the primary ores extracted, but iron ore was later discovered at deeper levels in 1984, and mining operations have continued to the present.

The H Iron Mine is developing an orebody that is classified as a skarn-type ore deposit. Based on genesis and mineralization characteristics, it was historically divided into three ore bodies: the western, eastern, and magnetite bodies. Currently, mining is focused on the magnetite body beneath the western ore zone. The western and eastern bodies were previously mined for lead and zinc. Given that landslides and surface collapse occurred within the western ore zone, where lead and zinc extraction once took place, relevant historical mining data were collected and analyzed.

Topographically, the Mt. Yemi area features a prominent east-west ridge centered on the 989.2 m peak. South of the ridge, the slopes are steep, whereas to the north, they are more moderate, reflecting rugged mountainous terrain. These slope characteristics correspond to the distribution of underlying bedrock: sandstone and shale dominate the northern side, while limestone constitutes the majority of the southern slope.

Since a major slope failure occurred in 2010, the Mt. Yemi area has experienced two additional slope failures, three sinkholes, and numerous tension cracks near the mountain summit. These developments have raised serious safety concerns for nearby residents and mine workers. Figure 12 shows an aerial photograph in 2017. Satellite imagery analysis revealed northeastward surface displacement due to the slope failures and sinkholes, while tension cracks occurred toward the southwest, opposite the direction of movement. This suggests a strong link between slope failure and surface collapse.

High-resolution drones with georeferencing capabilities were used to capture aerial photographs as shown in Figure 13, which were then employed to construct a 3D topographic model of the study area. This allowed for quantification of the size of the sinkholes and slope failure zones. The dimensions of the sinkholes were estimated as follows:

- Sinkhole 1: 48 m (long axis) × 40 m (short axis)
- Sinkhole 2: 73 m × 57 m

Figure 12. Aerial photo of ground subsidence area at Mt. Yemi

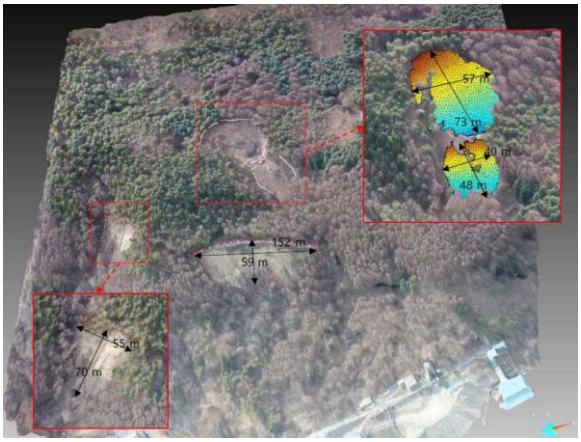

Figure 13. Dimensions of sinkholes and slope failure zones

For the slope failures:

- Slope failure 1: 55 m wide, 70 m in downslope length
- Slope failure 2: 152 m wide, 59 m in downslope length

Estimated volumes were:

- Sinkhole 1: 4,288 m³
- Sinkhole 2: 20,712 m³

Although the lateral expansion of Sinkhole 2 appears prominent, it is likely due to internal slope sliding within the sinkhole rather than ongoing surface subsidence. The combined volume lost beneath the surface, based on the difference between the original and current ground surfaces, is estimated at 25,000 m³.

Year-by-year analysis of aerial and satellite imagery indicates that subsidence and slope failures occurred sequentially and gradually expanded. This suggests that the subsidence did not occur into a pre-existing underground void. Rather, it likely developed as abandoned mine workings progressively collapsed and expanded toward areas containing fault breccias and karst cavities.

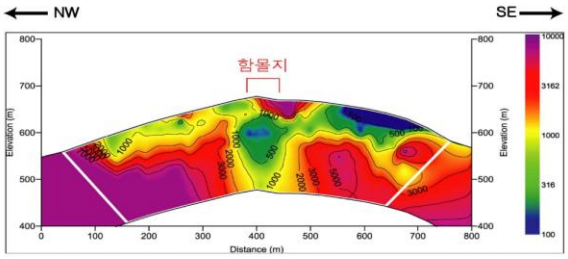

Figure 14. Line-3 electrical resistivity survey results for the Mt. Yemi case

The results from the Line-3 resistivity survey (Figure 14) reveal a distinct low-resistivity anomaly extending to depth beneath the central part of the sinkhole. This is attributed to the presence of a fault breccia zone, consistent with borehole investigations that identified core loss and fault breccia below the sinkhole. Furthermore, the lowest resistivity value—observed at the 600 m mark along Line-1—suggests the presence of a subsurface void responsible for triggering the surface collapse near the 600 m elevation.

A composite geospatial model was developed using drone imagery, 3D geological models, resistivity data, tunnel layouts, and field observations. The terrain surface was derived from a 1:5,000 digital elevation map published by the National Geographic Information Institute of Korea. Satellite imagery, aerial photos, and drone footage were draped over the topography to create a 3D visualization (Figures 15 to 17).

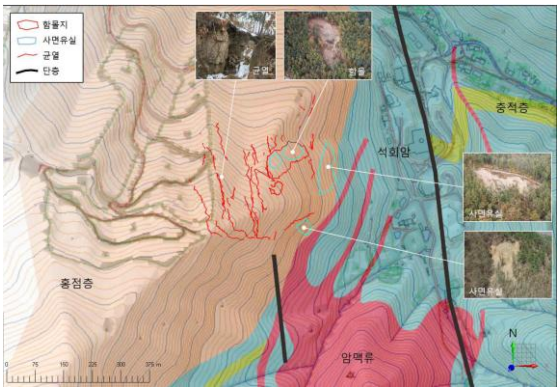

Figure 15. Composite model of the Yemi case

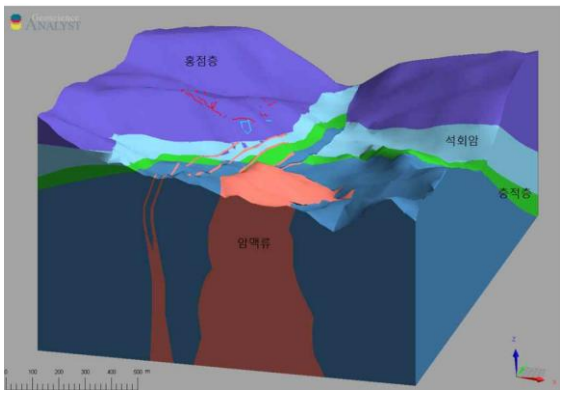

Figure 16. 3D geological model of the Yemi case

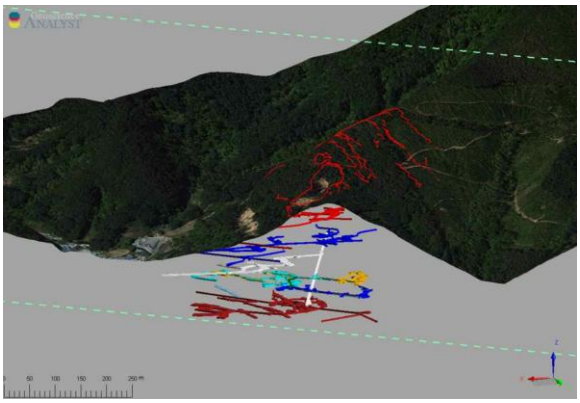

Figure 17. 3D distribution of mine tunnels at Yemi

In the Yemi case, a FLAC3D analysis was conducted, focusing on the distribution of plastic zones resulting from the application of the strength reduction method. The Mohr-Coulomb failure criterion was used, and cohesion, internal friction angle, and tensile strength were all reduced to simulate failure. Figure 18 compares the numerically predicted deformation zone with the actual hazard area. The mapped hazard area, based on field surveys, includes numerous tension cracks toward the south and west, which align well with the predicted deformation zone. This supports the conclusion that overall ground deformation induced by mined-out voids is closely related to the surface cracking observed.

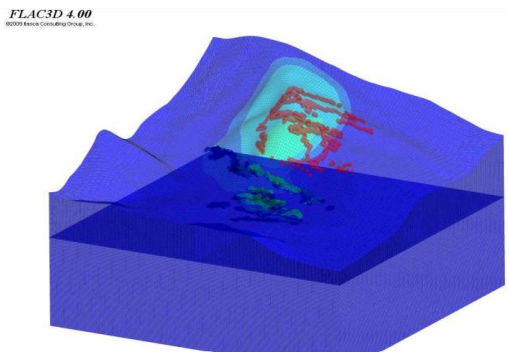

Figure 18. Influence zone of ground deformation induced by mined-out cavities at Mt. Yemi

These two cases collectively demonstrate that fault zones, karst cavities, weathered weak rock, and past mining activity are the key contributors to surface collapse. They also underscore the importance of site-specific investigation and monitoring strategies tailored to each site's unique failure mechanism.

4. Interpretation and Discussion

The two cases presented in this study demonstrate that while the failure patterns differ, collapses in fault-affected weak limestone rock masses can both pose serious geohazards. In both the Uljin and Yemi cases, ground collapses were triggered by a combination of faults, karstic features, weathering, and past mining activities.

In the Uljin subsidence case, analysis of the failure mechanism revealed the following:

- The surface subsidence manifested as a primary collapse depression accompanied by numerous tension cracks, which differs from the trough-shaped subsidence typically caused by over-excavation.
- The initial collapse occurred in transport tunnels used for mining the eastern and southeastern ore bodies, which required long-term operational stability. Thus, excessive mining in this zone is unlikely.
- Production records from the year prior to the collapse do not indicate a surge in extraction activity.

Collectively, these observations suggest no direct link between the Uljin ground subsidence and over-excavation.

Even in 3D numerical models assuming extreme production such as mass ore extraction, tunnel collapse was only predicted when unfavorable geological conditions were present—otherwise, no surface collapse developed. The geological investigation showed:

- The collapse originated near the boundary between bedded limestone and crystalline limestone, where weak rock was present.
- Clay-like materials were observed coating the tunnel roof, suggesting weathering due to rainwater infiltration, which likely reduced the shear strength of the rock.
- The surface displayed a typical collapse pattern: a large-scale depression, step-like subsidence, and circular cracks—indicating failure along a geological weak zone.

These findings confirm that weak geological structures, such as faults and karstic cavities, were primary contributors to the ground failure. Supporting this, 3D numerical models excluding weak zones predicted no collapse, while 2D models including them reproduced surface failure.

In the Yemi case, aerial photographs taken on May 8, 2011, revealed the initial sinkhole (Sinkhole 1), followed by the appearance of Sinkholes 2 and 3 in 2013. Sinkholes 1 and 2 were adjacent, while Sinkhole 3 was located approximately 20 meters south. Although Sinkhole 1 initially appeared larger, over time the affected area expanded such that, by 2017, the two formed a single depression with a total estimated collapsed volume of about 25,000 m^3. The terrain elevation varies by approximately 20 m between the southwest and northeast boundaries, due to the influence of the Mt. Yemi peak. The expansion of Sinkhole 2 toward the southwest appears to be caused not by new subsidence but by slope failure within the original sinkhole boundary. Sinkhole 3 has retained a near-circular shape.

The study examined the role of historical lead-zinc mining workings, based on the assumption that a large underground cavity is necessary to account for the observed volume of collapse (25,000 m^3). The analysis focused on the potential

presence of such cavities, their spatial relationship with the sinkholes, and their likelihood of collapse. It was found that:

- Old lead-zinc mine workings provided sufficient cavity volume.
- Overlying fault breccia and karst voids likely acted as conduits for the downward movement of collapsed material.

Thus, the historical mine workings were identified as the primary cause, while fault breccia zones and natural voids played secondary roles in facilitating the collapse. At least two large-scale abandoned workings were identified, and signs of roof collapse and rockfall confirmed the collapse mechanism.

4.1 Common Geological and Structural Features

Both cases shared the following geotechnical characteristics:

- Presence of severely weathered faulted limestone formations
- Unfilled, abandoned room-and-pillar or caving mine workings
- Extensive development of karstic voids and fault breccia zones
- Shallow cover between underground voids and the ground surface

These factors reduce cavity stability, promote stress concentration, and lead to progressive weakening of the rock mass. Electrical resistivity surveys proved to be effective in early identification of voids and fracture zones.

4.2 Distinct Collapse Patterns and Implications

The Uljin case involved gradual subsidence, with visible warning signs such as surface cracks, allowing for partial monitoring. In contrast, the Yemi case involved a rapid slope collapse without clear precursors—highlighting the limitations of surface-based investigations. Therefore,

- In zones of progressive subsidence, continuous drone monitoring, ground instrumentation, and predictive numerical modeling are essential.
- In areas at risk of sudden collapse, preemptive engineering measures such as cavity backfilling, cutoff wall installation, and slope reinforcement are required.

4.3 Technical Implications for Weak Rock Hazard Assessment

This study offers the following technical insights:

- Integrated analysis of geological surveys, borehole data, geophysical surveys, and mining records is necessary.
- Quantitative assessment of weak rock properties—e.g., cohesion, internal friction angle, and karstic features—is critical.
- Numerical modeling should include stress redistribution behavior in fault zones and cavities.

Technologies such as drones, electrical resistivity surveys, and inclined drilling can be used effectively.

4.4 Applicability and Future Directions

With the expansion of urban areas and increased use of underground space, managing risks in abandoned mine sites and carbonate terrains is becoming increasingly important. Going forward:

- A quantitative risk index integrating structural, geological, and anthropogenic factors should be developed.
- Advancements in time-series surveys and AI-based anomaly detection are needed.
- Establishing design guidelines for minimum cover thickness, fault offset distances, and cavity-based hazard zoning is essential.
- Community engagement and policy support based on local participation must accompany technical progress.

To reduce uncertainty in weak rock hazards, technical innovation must be supported by regulatory frameworks and educational initiatives.

5. Concluding Remarks

This study has examined two representative cases of soft rock hazards in faulted limestone terrains influenced by historical mining activity in South Korea. Through a combination of surface surveys, geophysical methods, borehole investigations, laboratory testing, and historical data analysis, the research provides a comprehensive understanding of the failure mechanisms involved in both progressive subsidence and sudden slope collapse.

The findings emphasize the complex interplay between geological conditions—such as faulting, karstification, and weathering—and anthropogenic disturbances in the form of abandoned room-and-pillar excavations. In both cases, the soft rock formations exhibited characteristics of reduced strength, discontinuity propagation, and low overburden support, all of which contributed to collapse susceptibility.

Case A at Uljin demonstrated a gradual deformation process with visible warning signs, enabling preemptive monitoring. In contrast, Case B at Yemi Mountain revealed the more unpredictable nature of shallow collapses in highly weathered, faulted carbonate slopes. These differences highlight the necessity of site-specific hazard assessment strategies tailored to the prevailing geological and structural conditions.

The study underscores the importance of integrating geotechnical, geophysical, and historical mining data to inform risk assessment and mitigation design. The effective use of drone photogrammetry, electrical resistivity tomography, and inclined borehole drilling proved especially useful in identifying critical weak zones and guiding investigation priorities.

From a broader perspective, the insights gained from these Korean case studies are highly relevant to other regions experiencing similar geotechnical conditions. As urban

development increasingly overlaps with legacy mining areas and tectonically active zones, the need for robust frameworks for soft rock hazard identification, early detection, and mitigation will continue to grow.

Future work should focus on refining hazard classification schemes for soft rock environments, developing predictive models that incorporate time-dependent behavior and structural complexity, and establishing clearer engineering guidelines for safe development in such areas. Collaboration across geotechnical disciplines and continuous updates to regulatory policies will be key to addressing the evolving challenges posed by soft rock hazards

Acknowledgments

This presentation is based on the reports by KIGAM (2017) and KOMIR (2019). The author would like to express sincere gratitude to Korea Mine Reclamation and Mineral Resources Corporation (KOMIR) and OO Corporation for their support in enabling the investigation to be conducted through the Korean Society for Rock Mechanics (KSRM) and the Korea Institute of Geoscience and Mineral Resources (KIGAM).

References

Kim, J.-W., Kim, M.-S., Lee, D.-G., Park, C., Cho, Y.-D., & Park, S.-K. (2014). Stability analysis of mine tunnels using laboratory tests and field rock mass classification. *Tunnel and Underground Space*, 24(3), 212–223. (in Korean)

Moon, Y.-H., Kwon, S.-J., Park, Y.-S., & Kim, M.-S. (2002). Detailed investigation report (Cheol and Yemi area). *Korea Resources Corporation*, pp. 1–55. (in Korean)

Jeon, B., Jeong, H.-Y., Choi, S., Jeon, S. (2022). Assessment of Subsidence Hazard in Abandoned Mine Area Using Strength Reduction Method. *KSCE Journal of Civil Engineering*, 26, 4338-4358.

Jeon, S., Jeon, B. (2014). Review on the Prevention and Reclamation of Mining Induced Subsidence in Abandoned Mine Areas in the Republic of Korea. *Journal of Korean Society of Mineral and Energy Resource Engineers*, 51(1), 141-150. (in Korean)

Jung, Y.-B., Song, W.-K., & Kang, S.-S. (2008). Development of a ground subsidence risk assessment method based only on tunnel depth information. *Tunnel and Underground Space*, 18(4), 272–279. (in Korean)

Coal Industry Rationalization Project Report, 04-12 (2004). A comprehensive analysis and future direction for ground subsidence prevention projects in abandoned mine areas. (in Korean)

Korea Institute of Geoscience and Mineral Resources (KIGAM). (2017). Detailed safety inspection report on ground subsidence area in the Uljin limestone mine. (in Korean)

Korea Mine Reclamation Corporation (KOMIR). (2019). Study report on the causes of surface subsidence and slope failure and establishment of safety measures in Mt. Yemi area. (in Korean)